

Localization and interaction of indirect excitons in GaAs coupled quantum wells

A. A. High,¹ A. T. Hammack,¹ L. V. Butov,¹ L. Mouchliadis,² A. L. Ivanov,² M. Hanson,³ and A. C. Gossard³

¹Department of Physics, University of California at San Diego, La Jolla, CA 92093-0319

²Department of Physics and Astronomy, Cardiff University, Cardiff CF24 3AA, United Kingdom

³Materials Department, University of California at Santa Barbara, Santa Barbara, California 93106-5050

(Dated: October 31, 2018)

We introduced an elevated trap technique and exploited it for lowering the effective temperature of indirect excitons. We observed narrow photoluminescence lines which correspond to the emission of individual states of indirect excitons in a disorder potential. We studied the effect of exciton-exciton interaction on the localized and delocalized exciton states and found that the homogeneous line broadening increases with density and dominates the linewidth at high densities.

PACS numbers: 73.63.Hs, 78.67.De

Disorder is an intrinsic feature of solid state materials. It forms due to the spatial inhomogeneity of the sample. In other systems, such as liquid Helium or cold atomic gases, disorder can be artificially introduced. The behavior of particles in a disorder potential is a subject of intensive research. The studies have concerned electrons in semiconductors and superconductors, liquid Helium in a porous media, and cold atomic gases in a disorder potential formed by optical patterning, see e.g. [1, 2, 3, 4, 5].

Understanding the role of disorder is also essential in the physics of excitons. For excitons in QW structures, the in-plane disorder potential forms mainly due to QW width and alloy fluctuations [6, 7, 8, 9, 10, 11]. Indirect excitons in coupled quantum wells (CQW) composed of an electron and a hole in separated QWs, Fig. 1a, form a peculiar system for studying the effects of disorder. While regular excitons are neutral particles and interact only weakly, indirect excitons are electric dipoles with dipole moment $d \approx L_z$, the distance between the QW centers, and interact as dipoles, $U_{int}(r) = e^2 d^2 / (\epsilon r^3)$, $r \gg d$ [12, 13, 14, 15]. The interaction should have a significant effect on the localization and transport of excitons in a disorder. Furthermore, the lifetime of indirect excitons exceeds by orders of magnitude the lifetime of regular excitons and indirect excitons can travel over large distances within their lifetime [16, 17, 18] facilitating the study of exciton transport by imaging spectroscopy. Also, due to their long lifetime, the indirect excitons can cool to temperatures close to the lattice temperature [19], permitting the study of cold excitons.

In this paper, we introduce an elevated in-plane trap technique facilitating the observation of individual exciton states in the disorder potential and present studies of the effect of interaction on indirect excitons in a disorder.

An in-plane trap was created by a pattern of electrodes, Fig. 1b. An electric field F_z perpendicular to the QW plane results in the exciton energy shift $\delta E = eF_z d$, Fig. 1d. The laterally modulated electrode voltage $V(x, y)$ creates an in-plane relief of the exciton energy $E(x, y) = eF_z(x, y)d \propto V(x, y)d$ [20]. CQW structure was grown by MBE. n^+ -GaAs layer with $n_{Si} = 10^{18} \text{ cm}^{-3}$ serves as a

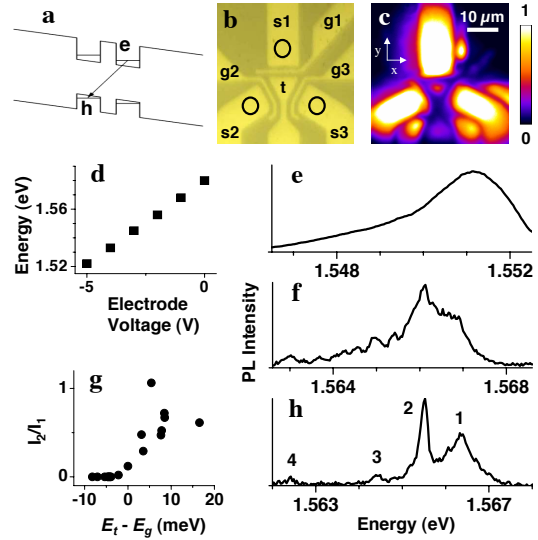


FIG. 1: (a) Energy band diagram of the CQW structure; e, electron; h, hole. (b) Electrode pattern. A trap is formed at electrode t by voltages on electrodes s , g , and t . The circles show the positions of the laser excitation. (c) Image of the indirect exciton emission in the elevated trap regime. $V_s = -2\text{V}$, $V_g = -1.5\text{V}$, $V_t = -0.5\text{V}$, $P_{ex} = 750 \mu\text{W}$. (d) Energy of the indirect excitons vs electrode voltage. (e) Emission spectra of indirect excitons in the normal trap. $V_s = -2\text{V}$, $V_g = -2.5\text{V}$, $V_t = -3.5\text{V}$, $P_{ex} = 18 \mu\text{W}$. (f) Emission spectra of indirect excitons in the normal trap for defocused laser excitation. $V_s = 0$, $V_g = 0$, $V_t = -0.5\text{V}$. $P_{ex} = 74 \mu\text{W}$ defocused over 0.1 mm^2 . (g) Ratio of line 2 to line 1 intensities vs energy difference of the indirect excitons in the trap t and surrounding gates g . $P_{ex} = 18 \mu\text{W}$. (h) Emission spectra of indirect excitons in the elevated trap. $V_s = -2\text{V}$, $V_g = -1.5\text{V}$, $V_t = -0.5\text{V}$, $P_{ex} = 18 \mu\text{W}$. $T = 1.4\text{K}$.

homogeneous bottom electrode. The electrodes on the surface of the structure were fabricated by depositing a semitransparent layer of Pt (8 nm) and Au (2 nm). Two 8 nm GaAs QWs separated by a 4 nm $\text{Al}_{0.33}\text{Ga}_{0.67}\text{As}$ barrier were positioned $0.1 \mu\text{m}$ above the n^+ -GaAs layer within an undoped $1 \mu\text{m}$ thick $\text{Al}_{0.33}\text{Ga}_{0.67}\text{As}$ layer. Positioning the CQW closer to the homogeneous electrode

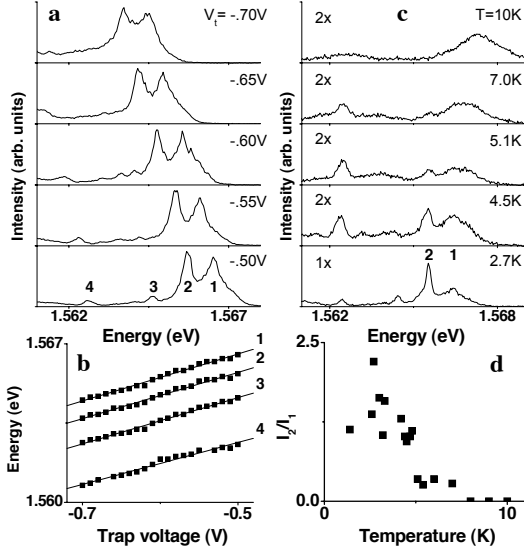


FIG. 2: (a) PL spectra of excitons in the elevated trap and (b) energies of lines 1-4 vs V_t . $V_s = -2V$, $V_g = -1.5V$, $T = 1.4K$, $P_{ex} = 18\mu W$. (c) PL spectra of excitons in the elevated trap vs bath temperature. $V_s = -2V$, $V_g = -1.5V$, $V_t = -0.5V$, $P_{ex} = 18\mu W$. (d) The ratio of line 2 intensity to line 1 intensity vs bath temperature. $V_s = -2V$, $V_g = -1.5V$, $V_t = -0.5V$, $P_{ex} = 6.3\mu W$.

suppresses the in-plane electric field, which otherwise can lead to the exciton dissociation [21]. The excitons were photoexcited by a 633 nm HeNe laser focused to a spot $\sim 5\mu m$ in diameter in the area shown by the upper circle in Fig. 1b [22]. The emission images were taken by a CCD with an interference filter 790 ± 5 nm, which covers the spectral range of the indirect excitons. The spatial resolution was 2 microns. The spectra were measured using a spectrometer with resolution 0.18 meV.

The electrode pattern shown in Fig. 1b was used to create normal traps at $|V_t| > |V_g|, |V_s|$ as well as elevated traps at $|V_t| < |V_g|, |V_s|$ for the indirect excitons in the region of central electrode t . The cloud of indirect excitons in the trap is in the center of Fig. 1c. In the normal trap the energy of the indirect excitons is below the energy of the surrounding areas, $E_t < E_g, E_s$, while in the elevated trap it is above $E_t > E_g, E_s$. For the entire range of the studied densities ($P_{ex} = 1 - 1140\mu W$ with the smallest limited by the signal strength) the emission spectrum in the normal trap was a structureless line with FWHM > 1 meV, like that in Fig. 1e. However, sharp lines were observed in the emission spectrum in the elevated trap, Fig. 1h. The sharp lines emerge at the transition from the normal trap to elevated trap, Fig. 1g.

FWHM of lines 2-4 were measured as low as 0.18 meV, which is close to the spectrometer resolution. Sharp lines in the emission of excitons in QWs were observed in earlier studies [8, 9, 10]. They were attributed to the emission of excitons localized in the local minima

of the disorder potential. The earlier reported sharp lines correspond to the emission of direct excitons with both electrons and holes confined in one QW. However, varying the electrode voltage V_t results in the energy shift of lines 1-4, Fig. 2a,b. The measured energy shift $\delta E \approx 10.4V_t$ meV/V corresponds to $d \approx 10.7$ nm, which is close to the nominal distance between the QW centers. Therefore, lines 1-4 correspond to the emission of the indirect excitons.

We attribute the low energy lines 2-4 to the emission of the exciton states localized in local minima of the disorder potential and the highest energy line 1 to the emission of excitons delocalized over the trap. The observation of the individual localized states in the disorder potential is facilitated by collecting the exciton emission from a small area, Fig. 1c, containing not too many localized states so that their emission can be resolved. In general, particles in a weak disorder are delocalized while deep minima, which occur in the disorder potential, produce strongly localized states. The disorder potential in QW structures generally has a broad distribution of lengths and depths [6, 7, 8, 9, 10, 11]. Localized and delocalized states can be distinguished via a different density dependence of their emission, as described below.

Utilizing an elevated trap leads to an effective “cooling” of the excitons. Since the energy of excitons in the elevated trap is higher than in the surrounding areas, excitons can escape the trap. The escape rate of excitons with a lower energy is generally slower. This increases the relative occupation of the lower energy states and, therefore, can be considered as lowering the exciton temperature. This mechanism of “cooling” has similarities with evaporative cooling. The “cooling efficiency” can be quantified by the relative populations of the localized and delocalized states. One can introduce an effective temperature \tilde{T} for the population balance between these states as $\delta = n_{deloc}/n_{loc} \sim \exp[-\varepsilon/(k_B\tilde{T})]$, where ε is a localization energy. Then the “cooling efficiency” in the elevated trap regime can be presented by the parameter $\gamma = \delta_{norm}/\delta_{elev}$. A large γ observed in the experiments indicates an efficient cooling. In turn, the temperatures in the elevated trap regime and in the normal trap regime are related by $1/\tilde{T}_{elev} = 1/\tilde{T}_{norm} + (k_B/\varepsilon) \ln \gamma$. This allows a rough estimate for \tilde{T}_{elev} . Assuming $\gamma \gtrsim 10$ and $\varepsilon/k_B \sim 10K$ (correspond to line 2, Fig. 1) and $\tilde{T}_{norm} \sim 3K$ (corresponds to a typical temperature of the indirect excitons in the presence of cw excitation and without the “cooling” [19, 23]), one obtains $\tilde{T}_{elev} \lesssim 1.8K$.

The “cooling efficiency” γ can be estimated by using the rate equations for occupations of the localized and delocalized states at equilibrium, which result to $\gamma = 1 + \tau/\tau_{esc}$, where $\tau^{-1} = \Lambda^{-1}\tau_{loc}^{-1} + \tau_{opt}^{-1}$, $\Lambda^{-1} = (\Lambda_l + \Lambda_d)/\Lambda_l$, Λ_d (Λ_l) is the population rate of the delocalized (localized) states due to the laser excitation, τ_{opt} and τ_{loc} are the radiative and localization times of the delocalized excitons, and τ_{esc} is their escape time from the elevated

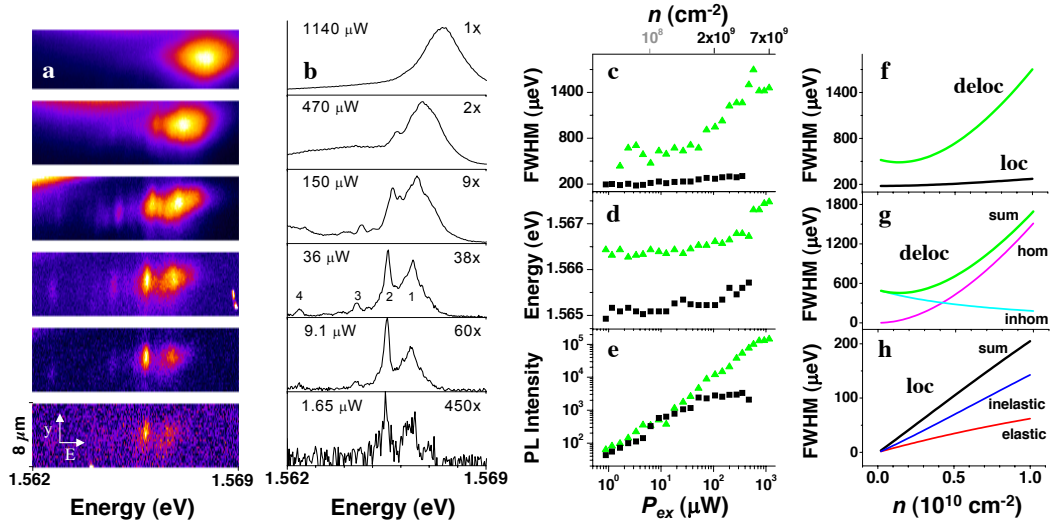


FIG. 3: (a) $E - y$ emission images and (b) spectra of indirect excitons in the elevated trap vs P_{ex} . (c) FWHM, (d) energy, and (e) intensity of line 1 (green triangles) and line 2 (black squares) vs P_{ex} . Density listed on top is an estimate based on the exciton energy shift, the lowest value is an estimate based on the PL intensity ratio. $V_s = -2V$, $V_g = -1.5V$, $V_t = -5V$, $T = 1.4K$. (g) Calculated FWHM of emission line of delocalized indirect excitons (green). Thin lines present the contributions from homogeneous broadening due to exciton-exciton interaction (magenta) and inhomogeneous broadening due to disorder (cyan). The disorder amplitude $U^{(0)}/2 = 0.35$ meV corresponds to line 1. (h) Calculated FWHM of emission line of localized indirect excitons (black). Thin lines present the contributions from inelastic (blue) and elastic (red) exciton scattering. $\epsilon = 1.3$ meV that corresponds to line 2. (f) Calculated FWHM of emission lines including the resolution 0.18 meV for comparison with the experimental data in (c).

trap ($\tau_{esc} \sim S_{trap}/D_x \sim 0.1-1$ ns for the elevated trap area $S_{trap} \sim 1\mu m^2$, Fig. 1c, and the diffusion coefficient $D_x \sim 10 - 100$ cm²/s [17]). For direct excitons with a short lifetime $\tau_{opt} \sim 0.01 - 0.1$ ns, the cooling is inefficient. Indeed, in this case $\gamma < 1 + \tau_{opt}/\tau_{esc} \sim 1.1$. On the contrary, the cooling can be efficient for the indirect excitons with a long lifetime $\tau_{opt} \sim 10 - 10^4$ ns. In this case $\gamma \sim 1 + \Lambda\tau_{loc}/\tau_{esc}$. It reaches $\gamma \sim 10$ estimated from the experiments when $\tau_{esc} \sim 0.1\Lambda\tau_{loc}$.

Note also that in the normal trap regime, the excitons created by the laser excitation in the region of electrode s travel to the trap following a downhill potential energy gradient. As shown in [23] traveling downhill may increase the exciton temperature. However, this heating mechanism is absent in the elevated trap regime [24]. The lower effective exciton temperature in the elevated trap compared to that in the normal trap facilitates the emergence of the lower energy lines in the elevated trap regime, Fig. 1g,e,h. Note also that the relative intensity of the lower energy lines 2-4 in the elevated trap regime reduces with increasing bath temperature, Fig. 2c,d.

We also performed an experiment at conditions in between these regimes: We studied excitons in the normal trap using defocused excitation, Fig. 1f. At these conditions, a significant fraction of the excitons is created in the trap. Therefore the heating due to the downhill travel present in a normal trap with remote excitation (Fig. 1e) is reduced yet the “cooling mechanism” of the elevated trap (Fig. 1h) is absent. Sharp lines can be observed in

this regime; however, they are not as pronounced as in the elevated trap. The rest of the paper concerns the elevated trap regime where the sharp lines are more distinct.

The exciton energy increases with density due to the repulsive dipole-dipole interaction of the indirect excitons, Fig. 3d. The exciton density n can be estimated from the energy shift δE as $n = \epsilon\delta E/(4\pi e^2 d)$ [12, 13, 14, 15]. It is presented at the top in Figs. 3c-e. The energy shift of the localized states is close to that of the delocalized states.

The emission intensity of the localized excitons saturates as shown in Fig. 3e for line 2. The saturation indicates that only a finite number of excitons can occupy a local minimum of the disorder potential. For the minimum corresponding to line 2 this number appears to be one. Indeed, if a second exciton were added to the minimum, the energy of the exciton state in it would increase due to the repulsive interaction. Since the area of the minimum is small compared to the area of the entire trap, adding one more exciton should result to a significant increase of the exciton density in it and, in turn, to a sharp increase of the energy of the localized state. Since no such energy increase is observed, no more than one exciton can occupy the local potential minimum. This is consistent with the small estimated exciton localization length in the minimum $l_{loc} \sim \hbar/\sqrt{(2M_x\epsilon)} \sim 10$ nm, which does not exceed the exciton Bohr radius. The effect is similar to the Coulomb blockade for electrons. It is due

to the dipole-dipole repulsion of the indirect excitons.

The spectral width of the delocalized state emission is given by $\Delta_{\text{FWHM}} = [\Gamma_{\text{hom}}^2 + \Gamma_{\text{inhom}}^2]^{1/2}$, where $\Gamma_{\text{hom}} = \hbar/\tau_{x-x} + \hbar/\tau_{x-LA} + \hbar/\tau_{\text{rec}}$ is the homogeneous broadening due to exciton – exciton and exciton – phonon scattering and finite recombination lifetime and $\Gamma_{\text{inhom}} = \langle U_{\text{rand}} \rangle$ is the inhomogeneous broadening due to disorder, $\langle U_{\text{rand}} \rangle$ is the average amplitude of the CQW in-plane long-range disorder potential. For $n \gtrsim 10^8 \text{ cm}^{-2}$ relevant to the experiments, $\Gamma_{\text{hom}} \simeq \hbar/\tau_{x-x}$ with τ_{x-x} given by

$$\frac{1}{\tau_{x-x}} = \left(\frac{u_0 M_x}{2\pi} \right)^2 \left(\frac{k_B T}{\hbar^5} \right) e^{-T_0/T} F_0 \int_0^\infty du \int_0^{2\pi} d\phi \frac{e^{2u}}{\left[e^{u(1-\cos\phi)} - F_0 \right] \left[e^{u(1+\cos\phi)} - F_0 \right] \left[e^{2u} - F_0 \right]}, \quad (1)$$

where $F_0 = 1 - e^{-T_0/T}$, $T_0 = \pi\hbar^2 n / (2M_x)$, and u_0 is approximated by $u_0 \simeq 4\pi e^2 d / \epsilon$ [25]. $\Gamma_{\text{inhom}}(n)$ evaluated with Eq. (1) is shown in Fig. 3g.

The inhomogeneous broadening is dominant at low densities where the interaction effects vanish. It produces a linewidth of 0.5 meV for the studied sample, Fig. 3c. The inhomogeneous broadening decreases with increasing density due to screening of the long-range disorder potential by interacting indirect excitons as

$$\Gamma_{\text{inhom}} = \frac{U^{(0)}}{1 + [(2M_x)/(\pi\hbar^2)](e^{T_0/T} - 1)u_0}, \quad (2)$$

where $U^{(0)} = 2\langle |U_{\text{rand}}(\mathbf{r}_1)| \rangle$ is the amplitude of the unscreened disorder potential, when $n \rightarrow 0$ [15]. $\Gamma_{\text{inhom}}(n)$ evaluated with Eq. (2) is shown in Fig. 3g.

The density increase also results in the homogeneous broadening of the localized states, lines 2-4 (Fig. 3c), due to the scattering of the localized exciton with delocalized excitons. It is given by $\Gamma_{\text{hom}}^{(\text{loc})} = \hbar/\tau_{\text{in}} + \hbar/\tau_{\text{el}}$ with

$$\frac{\hbar}{\tau_{\text{in}}} = \left(\frac{u_0 M_x}{2\pi\hbar^2} \right)^2 k_B T (1 + F_0) F_0 \int_{2\Delta}^\infty du \int_0^{2\pi} d\phi \frac{e^{2u}}{\left[e^{u-\Delta-f(u)\cos\phi} - F_0 \right] \left[e^{u-\Delta+f(u)\cos\phi} - F_0 \right] \left[e^{2u} - F_0 \right]}, \quad (3)$$

$$\frac{\hbar}{\tau_{\text{el}}} = \left(\frac{u_0 M_x}{2\pi\hbar^2} \right)^2 k_B T F_0 \int_0^\infty du \int_0^{2\pi} d\phi \frac{e^{u/\cos 2\phi}}{\left[e^{u/\cos 2\phi} - F_0 \right] \left[e^{u \tan 2\phi} - F_0 \right]}, \quad (4)$$

where $f(u) = \sqrt{u(u-2\Delta)}$ and $\Delta = \epsilon/(2k_B T)$. The first (second) contribution is due to the inelastic (elastic) scattering channel “localized exciton + delocalized exciton \rightarrow delocalized (localized) exciton + delocalized exciton”. In elastic scattering the delocalized exciton changes its momentum by the amount which can be relaxed by the localized exciton, $\sim 1/l_{\text{loc}}$. Both the experimental data,

Figs. 3c, and numerical evaluations with Eqs. (1),(3),(4), Fig. 3g,h, show that the homogeneous broadening of the localized state is smaller than that of the delocalized state. This difference can be attributed to the energy gap ϵ , which reduces the number of possible states for the scattering of localized excitons. This difference in linewidth broadening allows distinguishing the localized states from the delocalized states.

This work is supported by ARO, DOE, NSF, WIMCS.

-
- [1] P.A. Lee, T.V. Ramakrishnan, Rev. Mod. Phys. **57**, 287 (1985).
 - [2] M. Ma, B.I. Halperin, P.A. Lee, Phys. Rev. B **34**, 3136 (1986).
 - [3] M.P.A. Fisher, P.B. Weichman, G. Grinstein, D.S. Fisher, Phys. Rev. B **40**, 546 (1989).
 - [4] J.D. Reppy, Physica B & C **126**, 335 (1984).
 - [5] L. Fallani, J. E. Lye, V. Guarrera, C. Fort, M. Inguscio, Phys. Rev. Lett. **98**, 130404 (2007).
 - [6] J. Hegarty, L. Goldner, M.D. Sturge, Phys. Rev. B **30**, 7346 (1984).
 - [7] T. Takagahara, Phys. Rev. B **31**, 6552 (1985).
 - [8] A. Zrenner, L. V. Butov, M. Hagn, G. Abstreiter, G. Böhm, G. Weimann, Phys. Rev. Lett. **72**, 3382 (1994).
 - [9] H.F. Hess, E. Betzig, T.D. Harris, L.N. Pfeiffer, K.W. West, Science **264**, 1740 (1994).
 - [10] D. Gammon, E.S. Snow, B.V. Shanabrook, D.S. Katzer, D. Park, Phys. Rev. Lett. **76**, 3005 (1996).
 - [11] R. Zimmermann, E. Runge, Phys. Stat. Sol. (a) **164**, 511 (1997).
 - [12] D. Yoshioka, A.H. MacDonald, J. Phys. Soc. Jpn. **59**, 4211 (1990).
 - [13] X. Zhu, P.B. Littlewood, M. Hybertsen, T. Rice, Phys. Rev. Lett. **74**, 1633 (1995).
 - [14] Yu.E. Lozovik, O.L. Berman, JETP Lett. **64**, 573 (1996).
 - [15] A.L. Ivanov, Europhys. Lett. **59**, 586 (2002).
 - [16] M. Hagn, A. Zrenner, G. Böhm, G. Weimann, Appl. Phys. Lett. **67**, 232 (1995).
 - [17] A.L. Ivanov, L.E. Smallwood, A.T. Hammack, Sen Yang, L.V. Butov, A.C. Gossard, Europhys. Lett. **73**, 920 (2006).
 - [18] A. Gartner, A.W. Holleitner, J.P. Kotthaus, D. Schul, Appl. Phys. Lett. **89**, 052108 (2006).
 - [19] L.V. Butov, A.L. Ivanov, A. Imamoglu, P.B. Littlewood, A.A. Shashkin, V.T. Dolgoplov, K.L. Campman, A.C. Gossard, Phys. Rev. Lett. **86**, 5608 (2001).
 - [20] T. Huber, A. Zrenner, W. Wegscheider, M. Bichler, Phys. Stat. Sol. (a) **166**, R5 (1998).
 - [21] A.T. Hammack, N.A. Gippius, Sen Yang, G.O. Andreev, L.V. Butov, M. Hanson, A.C. Gossard, J. Appl. Phys. **99**, 066104 (2006).
 - [22] Results of experiments with three excitation spots at the three circles in Fig. 1b were qualitatively similar.
 - [23] A.T. Hammack, M. Griswold, L.V. Butov, L.E. Smallwood, A.L. Ivanov, A.C. Gossard, Phys. Rev. Lett. **96**, 227402 (2006).
 - [24] Traveling uphill may reduce the exciton temperature in the elevated trap that is opposite to the case of the downhill traveling. However, in the presented experiments this is inessential since the estimated number of excitons which can overpass the potential energy hill and reach the

elevated trap is small compared to that of excitons created in the trap due to the tails of the laser excitation.

[25] A.L. Ivanov, P.B. Littlewood, H. Haug, *Phys. Rev. B* **59**,

5032 (1999).